AUTHOR(S): IYI, D., HASAN, R. and PENLINGTON, R.

TITLE: Experimental and numerical study of buoyancy-driven low turbulence flow in rectangular enclosure partially filled with isolated solid blockages.

YEAR: 2018

Publisher citation: IYI, D., HASAN, R. and PENLINGTON, R. 2018. Experimental and numerical study of buoyancy-driven low turbulence flow in rectangular enclosure partially filled with isolated solid blockages. International journal of heat and mass transfer [online], 127(Part B), pages 534-545. Available from: https://doi.org/10.1016/j.ijheatmasstransfer.2018.07.031

OpenAIR citation: IYI, D., HASAN, R. and PENLINGTON, R. 2018. Experimental and numerical study of buoyancy-driven low turbulence flow in rectangular enclosure partially filled with isolated solid blockages. International journal of heat and mass transfer, 127(Part B), pages 534-545. Held on OpenAIR [online]. Available from: https://openair.rgu.ac.uk/

Experimental and Numerical Study of Buoyancy-driven Low Turbulence flow in Rectangular Enclosure Partially Filled with Isolated Solid Blockages

Draco Iyi[1], Reaz Hasan[2], Roger Penlington[3]

[1]Department of Mechanical Engineering, School of Engineering
Robert Gordon University Aberdeen, AB10 7GJ, United Kingdom
Phone: +44 (0) 1224 262412; Email: d.iyi@rgu.ac.uk

[2-3]Department of Mechanical and Construction Engineering
Faculty of Engineering and Environment
Northumbria University, Newcastle upon Tyne, NE1 8ST, United Kingdom

Abstract

This paper considers the natural convection inside an air filled enclosure having several isolated cylindrical blockages distributed within it, and arranged parallel to two vertical walls of the enclosure. These two walls are maintained at different temperatures resulting in a natural convection process inside the enclosure. The objectives are to provide experimental temperature data and to investigate the influence of the blockages proximity within and outside the active vertical wall hydrodynamic boundary layer of the natural convection flow and heat transfer. Experiments were designed with high degree of accuracy to provide reliable temperature data-bank for a range of blockages proximity to the active vertical walls. The test enclosure is an air filled rectangular cavity fixed at 0.97 m × 0.4 m × 1 m, corresponding to the height, width and depth respectively. The top and bottom walls are conducting surface and the temperature difference between the active vertical walls was maintained at 42.2 °C resulting in a characteristic Rayleigh number of 4.04×10^9 based on the enclosure height. All the walls of the enclosure were insulated externally while the inner surfaces were covered with conducting plate. The test cavity capability of establishing low turbulence natural convection flows was verified. All temperature data were obtained at steady state and it was verified to be reproducible by repeating the experiment at different times. Also, two-dimensionality was verified via rigorous temperature readings over a period of time. Additional temperature readings were recorded for the air and cylinder surfaces at several distinct locations. Further investigations were conducted using a numerical approach to supplement and validate the experiments.

Experimental temperature data collated at various locations within the enclosure show excellent comparison with numerical results and as such provide a useful experimental benchmark temperature data for the validation of low turbulence natural convection flow in enclosure partially filled with isolated solid objects. Our result shows that a significant increment or reduction in air temperature and wall heat transfer could be achieved by varying the blockages proximity, and especially when the blockages are positioned within the hydrodynamic boundary layers of the active vertical walls.

Keywords: Buoyancy-driven flow, isolated blockages, experimental benchmark data, numerical study, heat transfer, natural convection flow.

Nomenclature

C_p	specific heat at constant pressure, J/(kg-K)
D	depth of the cavity, m
g	gravitational acceleration, m/s^2
H	height of the cavity, m
$\overline{k}$	average thermal conductivity, W/(mK)
L	width of the cavity, m
Nu	local Nusselt number, $= Q_i L / \left(\overline{k} \Delta T\right)$
$\overline{Nu}$	average Nusselt number, $= \overline{Q} L / \left(\overline{k} \Delta T\right)$
$\Delta \overline{Nu}$	change in average Nusselt number, $= \overline{Nu}_\delta - \overline{Nu}_f$
$\% \Delta \overline{Nu}$	percentage change in average Nusselt number, $= 100 \times \Delta \overline{Nu} / \overline{Nu}_f$
Q	local heat flux, W/m^2
$\overline{Q}$	integral average heat flux, W/m^2
f	empty enclosure (Reference cavity)
δ	blockages proximity from active vertical wall
Ra_L	Rayleigh number, $= g\beta\left(T_{hot} - T_{cold}\right)L^3 / \left(\alpha\nu\right)$
Ra_H	Rayleigh number based on height, $= g\beta\left(T_{hot} - T_{cold}\right)H^3 / \left(\alpha\nu\right)$
T	temperature (K, °C)
T^*	non-dimensional temperature, $= \left(T - T_{cold}\right) / \Delta T$
ΔT	temperature difference, $= T_{hot} - T_{cold}$
$u*$	near-wall velocity, $= C_\mu^{1/4} k^{1/2}$
v_x	fluid velocity component in x-direction, m/s
v_y	fluid velocity component in y-direction, m/s
x, y, z	Cartesian coordinates
y^+	non-dimensional wall distance, $= \left(u * \Delta y\right) / \nu$
Δy	distance to the nearest wall

Greek symbols

α	thermal diffusivity, m^2/s
β	thermal expansion coefficient, (1/K)
ε	turbulent dissipation rate, m^2/s^2; Emissivity
ρ	fluid density, kg/m^3
μ	dynamic viscosity kg/m-s

1.0 **Introduction**

Buoyancy-driven flow and heat transfer in cavities partially filled with isolated solid products is important in the design of a wide range of industrial and engineering applications such as thermal management of indoor environments, cooling of electronic panels, drying of agricultural products and stacking of items in cold storage etc. The flow in such a confined space develops as a result of temperature gradient between two adjacent vertical walls of the cavity. The flow phenomenon has been the subject of extensive research due to its relevance in many practical applications [1, 2, 3]. As a result, there has been a growing demand for experimental data which will aid the development of more robust numerical method in order to achieve most approximate estimation of the transfer processes inside the cavity.

The basic set up for such flows that has also attracted most attention from researchers, is an air filled rectangular cavity without solid products whose opposing vertical walls is heated differentially [4, 5, 6, 7]. Detailed data on the flow, turbulence and wall heat transfer coefficients have been collected through various experiments [8, 9, 10].The experimental data available in literature have enabled the continuous development of numerical approach and methods by conducting validation and exploratory studies on this very topic [11]. The interest seems to be on-going because more challenging situations are emerging with time [12, 10]. In the case of a rectangular cavity of height H, the natural convection heat transfer from hot to cold walls is characterized by the formation of a slow moving vortex along the solid walls and the intensity of the flow can be conveniently expressed by the Rayleigh number [13, 12] as defined by Eq.(1). Depending on the Rayleigh number the flow can be treated as turbulent or laminar, where $Ra \le 10^8$ indicate buoyancy-induced laminar flow, with transition to turbulence occurring over the range of $10^8 \le Ra \le 10^{10}$ [14].

$$Ra = \frac{g\beta\left(T_h - T_c\right)L^3}{\nu\alpha} \qquad (1)$$

Another trend in buoyancy driven flow research has been focused on the examination of enclosures partially filled with solid products [15, 16, 17, 18, 19]. Similar to that of the empty cavity, the flows in such confined spaces develop as a result of temperature gradient but complicated by the interactive effects of the solid products which act as blockages (obstacles) to the airflow and heat transfer. Unlike porous media [18, 20, 15], these obstacles are not in contact with each other, but are close enough to influence the transfer processes inside the enclosure.

The majority of the studies in this category is based on the steady state laminar flow of Rayleigh number from 10^4 to 10^8. Typical example of studies in this category is the work by Das and Reddy [19], Defrayed and Lauriat [21] and Basak et al. 2006 [20], all of which are limited to steady state two-dimensional laminar natural convection flow of the Rayleigh number ranging from 10^5 to 10^8. Das and Reddy [18] and Yoon et al. 2010 [22] have reported the fluid flow and heat transfer in a differentially heated rectangular cavity containing just one disconnected solid product, while Bragas and de Lemos [23, 16], Hooman and Merrikh [17] investigated the cavity filled with several obstacles. The key findings from these research works show that when a limited number of solid products are involved, the fluid flow is predominantly confined between the vertical walls and the first column of the objects.

It is important to mention that investigations have been reported for an air-filled empty box [13, 9, 24]and box partially filled with isolated solid products [25, 23]. However, no study have been reported for isolated solid products arranged in clusters in such a way that it interact with the flow near the active vertical walls of the chamber. This configuration has its relevance either cold or warm storage and in the design and location of clustered heating elements, etc. The aim of this paper is therefore to explore the effect of isolated blockages proximity from the enclosure active vertical walls on the natural convection flow and heat transfer.

2.0 **Problem Description**

A natural convection experimental test rig whose flow domain is a rectangular box with a constant temperature gradient between the active vertical walls and conducting surface for both horizontal surfaces was designed and fabricated to obtain temperature data at various strategic positions within the enclosure. The test rig is capable of establishing low Rayleigh number natural convection flow inside the enclosure with or without the solid cylindrical blockages. The enclosure without blockages was used as a reference to that with blockages in order to quantify the influence of the blockages proximity from the active vertical wall. The enclosure flow domain size is fixed at 0.97 m high, 0.4 m wide and 1 m deep, with aspect ratios of AR_x= 2.425 (=H/L) and AR_y= 2.5 (=D/L). The temperature difference between the isothermal vertical walls was maintained at 42.2 °C. The Rayleigh number based on these dimensions and the temperature gradient between the active vertical walls was evaluated as 4.04 x 10^9, therefore a weak natural convection turbulent flow is expected inside the cavity. The schematic of the flow domain set-up for cavity with blockages is shown is Figure 1.

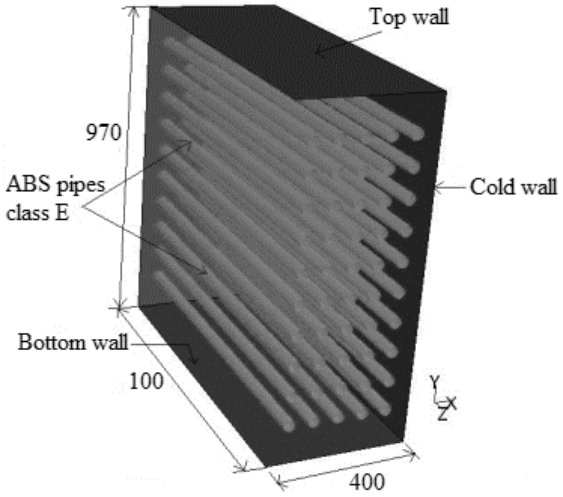

Figure 1: configuration of the flow domain (all dimension are in mm)

One of the key objectives of this paper is to provide high quality temperature benchmark data for the validation of numerical method. To achieve this, rigorous attempts were made to scrutinize various factors that are likely to influence the experimental conditions. The factors scrutinized are: the two-dimensionality of the flow domain at three cavity depths, the energy balance of the cavity, and uniformity of temperature distribution on the inner surface of the active vertical wall and the repeat of measurements for air temperature data at different locations within the fluid domain. After satisfactory temperature data were obtained for steady state situation, isolated cylindrical pipes (blockages) were systematically positioned inside the enclosure. With the same experimental conditions, the set up was left to run for 42 hours to allow the establishment of natural convection flow and temperature data were collated at steady state. The experimental temperature data were complemented by conducting detailed numerical simulations using experimental boundary conditions which enabled us to validate our experimental temperature data elsewhere in the domain. Further numerical investigations on the effect of blockages proximity to the active vertical walls on the natural convection flow and wall heat transfer coefficient was also conducted.

3.0 **Experimental Facility and Procedure**

The schematic of the thermal rig facility and set-up is depicted in Figure 2. The major components of the rig are the rectangular box, the active vertical walls (hot and cold wall) temperature control systems and facilities for gathering temperature data. A detailed description

of the experimental test rig design, validations and the temperature measurement are presented later. The following sections deal with the cavity design (which includes the description of the hot and cold walls and their temperature control mechanism) and technique for temperature measurement at various positions within the fluid domain and at the solid wall surfaces.

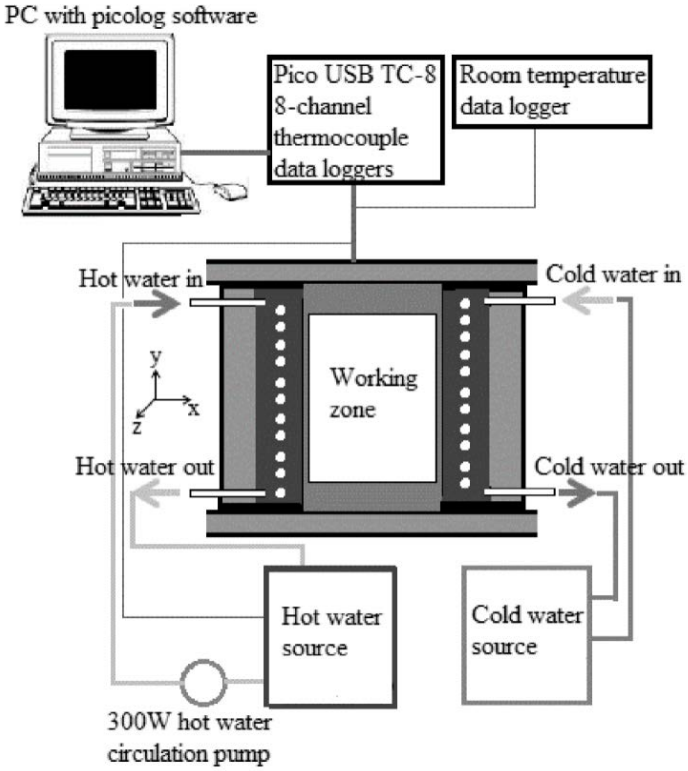

Figure 2: schematic of the experimental facility

3.1. **Test rig design and setup**

The rectangular enclosure is made up of active vertical walls (hot and cold walls), conducting horizontal walls (top and bottom walls) and two passive side walls. The internal surface of the enclosure was fitted with a low emissivity polished aluminum plate. The hot and cold isothermal surface of the cavity is made of heat exchangers embedded in a mold of epoxy plaster of thickness 40 mm. The surface facing the fluid domain is fitted with aluminum plate, while the other faces are insulated with 89 mm thick polystyrene (xtratherm) board. The polystyrene boards are gas tight foil facers (this makes the insulator air tight) and vapour resistant. Low emissivity of the foil gives its high thermal performance. All arrangements were guarded with wooden plates of thickness 6.35 mm. Both heat exchangers have been designed and fabricated in-house using 13 mm internal diameter copper tubes and fittings. To keep the losses through the gaps to a minimum, the joints between the four walls was fixed tightly to remove any gaps between the walls. All the four walls were clamped externally with a fixed steel frame with the side walls fixed with adjustable frame.

Hot and cold water at constant temperature was pumped through the heat exchanger of the hot and the cold walls respectively. A digitally controlled stirred heated circulating bath was used with a pump supply the constant temperature hot water. Cold water was supplied using a recirculation high flow rate chiller and pumped through the cold wall heat exchanger. The heat input device for the hot water bath was a 2 kW immersion heater, and hence has the capacity to supply the required energy for hot wall. To keep the temperature steady at ± 0.1 ^{0}C, a PID temperature controller was fitted to the heater to maintain the temperature of the hot water at

the set value. The PID controller provided proportional, integral and derivative control and was adjusted to automatically compensate for the temperature changes in the system.

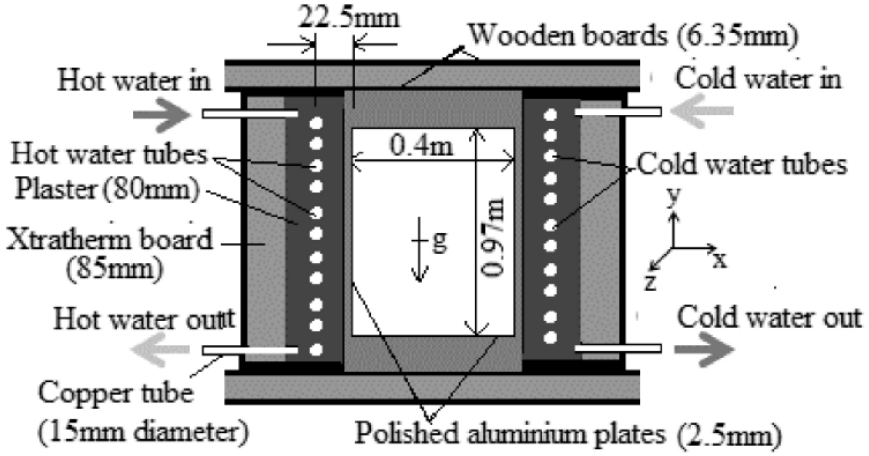

Figure 3: vertical section of test cavity arrangement

The design of the cold wall system is similar to that of the hot wall. The inlet and outlet of the cold wall heat exchanger were connected to a recirculation chiller. The plumbing connections are located on the rear of the unit and labeled as supply and return. The chiller is designed to provide a continuous supply of cooling water at a constant temperature and flow rate. The cooling capacity of the unit is 1 kW at 20 ^{0}C set point, with a temperature range of 4 ^{0}C to 35 ^{0}C. The water temperature of the inlet and the outlet of the radiator were measured using three type K thermocouples, for the inlet and outlet copper tubes. The thermocouples were connected to a PC through a USB based data acquisition system to monitor and record the temperatures at the selected sampling rate, which was set at every five seconds. Lab-calibrated 75 μm Chromel-Alumel, type-k thermocouples were used to measure all temperature data. A similar technique was used for the hot water system. The heat loss from the hot wall is the heat transfer to the enclosure structure and then through the cavity walls or to surrounding air through joints/gaps. The heat loss through the hot wall was evaluated and it was less than 1.5%. Therefore, this rig was able to give reliable temperature data.

All experiments were performed in an air-conditioned room with the ambient temperature kept at almost the same temperature as the average temperature value of the hot and cold walls (=44.4 ±0.8 °C). The temperature of the hot and cold wall was maintained isothermally at 65.5 ±0.8 °C and 23.3 ±0.8 °C respectively. The energy balance of reference (empty) enclosure was conducted and the heat transfer into the cavity from the hot and bottom walls was about 109.11 W and 23.38 W respectively. Also, the net heat gained by the cold and the top walls were about 111.35 W and 20.02 W respectively. The percentage difference between the heat transfer into the cavity and the heat the transfer out of the cavity is about 0.46%. Further information on the energy balance can be found in Draco [26].

3.2. **Enclosure partially filled with solid blockages**

As stated earlier, the major aim of this paper is to investigate the influence of blockages interactions with the natural convection wall bounded flow by varying its proximity from the active vertical walls. To achieve the above aim, the empty rectangular box test rig (Figure 3) was modified to contain arrays of disconnected cylindrical ABS pipes (acting as blockages to the flow and heat transfer within the enclosure), which were systematically stacked in 5 rows and 10 columns as shown in Figure 4. The cylinders were uniformly distributed inside the enclosure for each of the proximity values (δ values) used and the distance between cylinders adjacent to each other were uniformly varied accordingly. The diameter and length of the ABS pipes (blockages) were 33.7 mm and 1000 mm respectively, and its surface-fraction densities represent about 34.3% of the total fluid domain. ABS material was chosen because of its light

weight, rigidity, and its suitability for use over a wide range of temperature (-40 ^{0}C to +80 ^{0}C) and up to 15 bar pressure. The thermal coefficient of linear expansion of the blockages is $10.1\times10^{-5}/^0$C and its thermal conductivity and emissivity are 0.33 W/m-k and 0.9 respectively.

The low thermal conductance helps to maintain a uniform temperature when interacting with air and also helps to eliminate or reduce the need for pipe insulation to control sweating. The blockages were positioned linearly near the side walls using specially designed guide rails fitted to these walls. The guide rails were accurately fitted to the walls with the help of a digital height gauge of accuracy ±0.05 and resolution of 0.01 mm. The schematic is shown in Figure 4, with the thermocouple positions on the surface of the pipes P-1 (upper surface) and P-2 (lower surface).

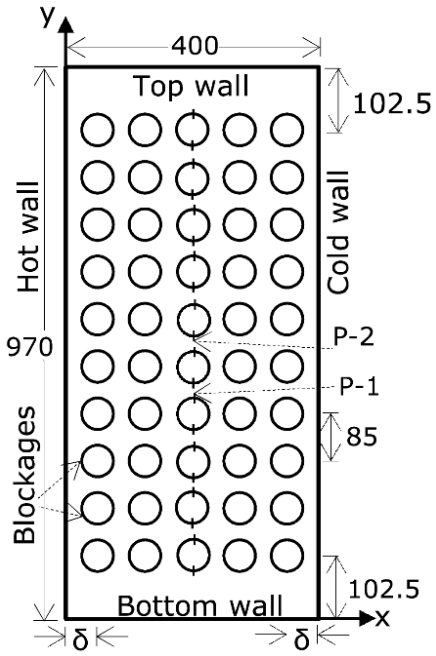

Figure 4: stacking of the blockages and thermocouples position on the cylinder wall surfaces

3.3. **Experimental calibrations**

Thermocouples used for all temperature measurements were carefully calibrated using a reference digital thermometer with the following specifications; model: CIS-640P, accuracy: ±0.1 ^{0}C, resolution: 0.01 ^{0}C, range: -50 ^{0}C to +200 ^{0}C, stability of 0.01 ^{0}C with a resolution of 0.01 ^{0}C and uncertainty of ±0.05 ^{0}C. The calibration of these thermocouples was done using the hot water tank with stirring devices which helped to keep the temperature of the water uniform. Three reference temperatures of 18 ^{0}C, 45 ^{0}C and 70 ^{0}C were used for the calibration. The thermocouple and the thermometer were immersed in a stirred water bath close to each other.

For each calibration case, the initial offset of temperature was equalized through the conversion equation based on type-k thermocouple within the data logging software. The measurement model for the thermocouple consists of a thermocouple placed in the medium being measured, thermocouple junction, thermocouple extension wire and data acquisition hardware and software. Throughout the calibration, the temperature of the thermocouple and that of the reference thermometer are assumed to be the same. Therefore, the uncertainty coming from this source should be about ±0.5 ^{0}C. Further information on the experimental uncertainty can be found in Draco Iyi [26].

To measure the air temperature, a digital height gauge of accuracy ±0.05 mm and resolution of 0.01 mm was used to measure the probe distance from the walls. All thermocouple probes

were positioned in the desired point with the help of a specially fabricated micro elastic spring fitted on the side walls. Therefore the uncertainty of the thermocouple probe position should be about than ±0.05 mm.

3.4. **Temperature distributions at the vertical walls**

The wall temperature distributions were measured at steady state conditions at various positions along the surface of the cold and hot wall. Table 1 shows the various positions with their corresponding temperatures. The purpose is to ensure that there are uniform temperature distributions at the surface of the active vertical walls. Thermocouples were fixed at three different positions along the horizontal direction from the edge of the side walls and at six different vertical positions from the bottom wall of the enclosure. The horizontal positions are 0.1 m, 0.2 m and 0.3 m, while the six positions along the vertical direction of the surfaces are 0.15 m, 0.35 m, 0.50 m, 0.65 m, 0.80 m and 0.90 m respectively.

The thermocouples were welded onto the desired position at each wall surface. To ensure position accuracy, the thermocouples were positioned using precision digital height gauge. Several attempts were made to ensure a uniform temperature distribution by adjusting the pump flow rate and moderating the hot and cold water supply temperatures. Average value of the most uniform wall temperature for the hot and cold walls were evaluated. For hot wall surface the average temperature was 65.5 °C (with a standard deviation of about 0.1833 and standard error of about 0.0432) and the cold wall surface was 23.3 °C (with standard deviation of 0.1085 and standard error of 0.0256). The above operating conditions and the wall average temperatures were used for all experiments reported in this paper. The surface emissivity value was measured using a thermal imaging camera (E60bx model) and was found to be 0.07, while the thermal conductivity of the material (202.4 W/m-K) was taken from table of material property.

Table 1: Wall temperature distributions data (°C)

	Hot wall			Cold wall		
	x_1	x_2	x_3	x_1	x_2	x_3
y_1	65.3	65.5	65.6	23.4	23.5	23.2
y_2	65.5	65.7	65.4	23.3	23.2	23.2
y_3	65.3	65.8	65.3	23.1	23.1	23.2
y_4	65.2	65.7	65.3	23.2	23.4	23.3
y_5	65.5	65.5	65.8	23.3	23.2	23.2
y_6	65.5	65.3	65.4	23.3	23.4	23.3

The temperature profile for the highly conductive top and bottom wall of the rectangular enclosure was initially examined at different vertical wall temperature gradients. The normalized temperature profiles measured along the horizontal wall surfaces from the heated vertical wall of the enclosure are represented by a best-fit linear curve shown in Figure 5. Since the horizontal walls are conducting surface, it is therefore expected that natural convection heat flow will propagate linearly along these surfaces due to the temperature difference between the hot and cold vertical walls. As the natural convection flow moved from the hot wall to the cold wall it dissipates (top wall) or absorb (bottom wall) some of the heat from the fluid near the surface due to conduction, convection and radiation transfer processes. As expected for a conduction horizontal surface, the trend in the temperature profiles shown in Figure 5gives a linear temperature profile from hot to cold wall along the surface.

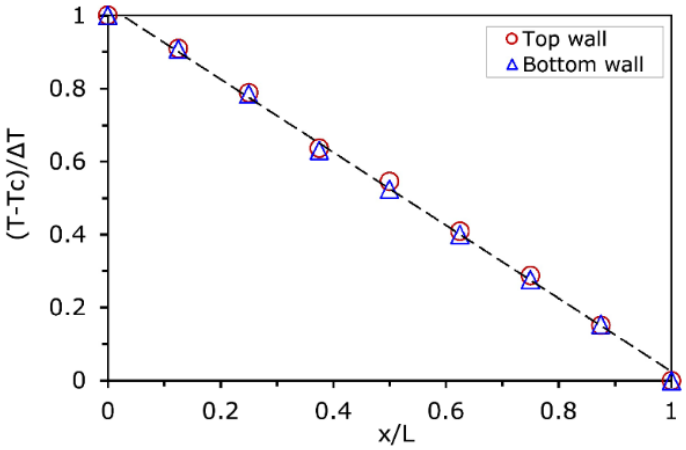

Figure 5: Temperature profile on horizontal walls

3.5. **Test rig validations**

The data measured in the experiments are limited to temperature only. This is because in natural convection flow phenomenon involving dry air, temperature is the most critical quantity due to the fact that it may be interpreted as both the cause and effect and vice versa. The natural convection flow developed due to buoyancy is directly dependent on temperature and at the same time the flow field is also affected by temperature.

Air temperature measurements at the same positions for each thermocouple was repeated over three different days and the collated temperature results were compared as shown in Figure 6(a). Also, two-dimensionality was thoroughly examined and verified as shown in Figure 6(b-d). The number of measurement sample points chosen was considered to be sufficient to give statistically significant profiles. The temperature profiles were measured across different sections of the cavity along the mid-width of the active walls and the number and location of these sections depends on the case being studied. Furthermore, one of the temperature measurements has typically been repeated over three different consecutive days to ascertain steady state conditions and repeatability of data. Figure 6(a) illustrates an example of one of the repeated measurements and it clearly shows that the experimental results can be reproducible. The average standard error was evaluated to be less than 0.21%, justifying the reliability of the test rig.

Two dimensional nature of the flow was verified by comparing the temperature distributions at three different sections of cavity depth, z/D =0.15, 0.5 and 0.85 and for three different horizontal planes, namely y/H= 0.05, y/H= 0.5 and y/H= 0.95. There is an excellent comparison between the temperature profiles of these three positions as shown in Figure 6(b-d). The maximum Standard error was about 0.206%and the average standard error is less than 0.1%. This indicates that the difference in the temperature data at the position is insignificant and therefore suggests that the cavity depth can provide a reliable 2D field. Ampofo and Karayiannis [13] and Betts and Bokhari [27] have acknowledged that the 2D approximation of experimental natural convection in cavities should be valid if the horizontal aspect ratio (D/L) of the cavity is greater than 1.8. The D/L value of our test rig is 2.8 which is a further vindication for 2D flows.

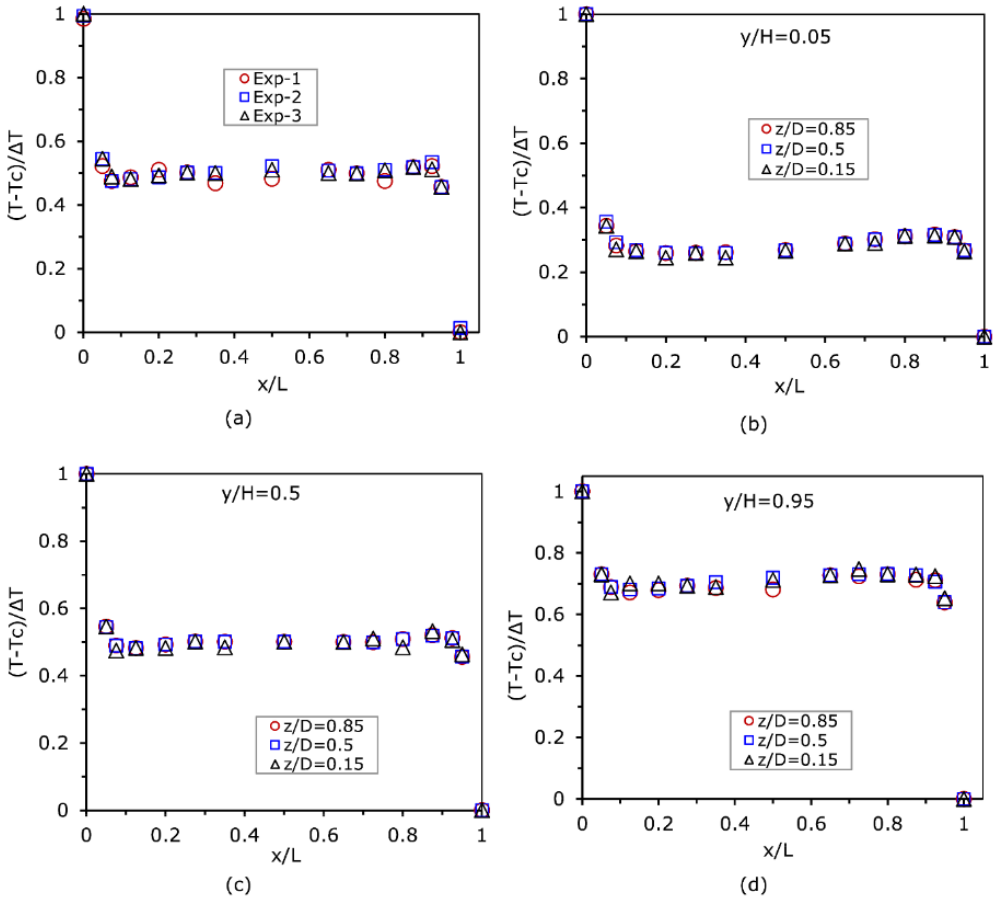

Figure 6: (a) repeatability of temperature measurements at mid-height for three different days. 2D verifications at three different cavity depths (b) near bottom wall (y/H= 0.05), (c) mid-height (y/H=0.5) (d) near top wall (y/H= 0.95)

4.0 **Experimental Temperature Benchmark Results**

Experimental benchmark data for air temperature collated at various locations inside the enclosure with and without blockages are presented in Figure 7(a-b). Experimental air temperature data at selected locations of the cavity with and without blockages have shown an excellent comparison with that of CFD simulations as presented later in Figure 9(a-d) and Figure 10(a-b). Overall, the experiment is carefully designed and tested to supply benchmark data for this type of natural convection flow setup conditions. Therefore, the experimental procedure and the measured temperature data could be used as a benchmark for the validation of CFD codes and the development/estimation of practical flows in an enclosure partially filled with isolated blockages/objects.

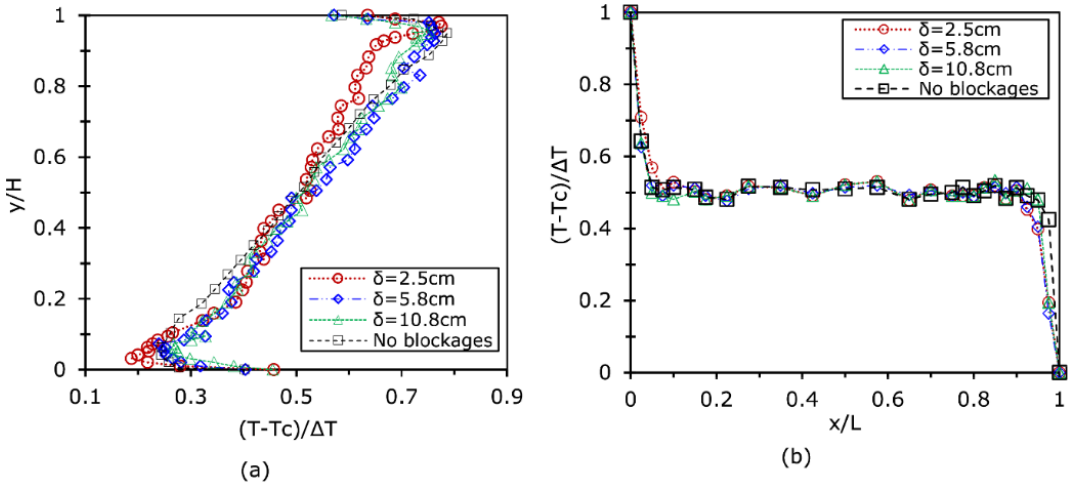

Figure 7: Dimensionless temperature at (a) mid-width (b) mid-height

5.0 **Numerical Procedure and Results**

The flow domain used in the numerical simulation is similar to that of the experimental setup shown in Figure 4. Numerical investigation was conducted for all test cases of blockages proximity as discussed earlier in section 3.2 using ANSYS FLUENT [28]. Turbulent fluxes of momentum, heat and mass were modelled by low Reynolds number k-ε eddy viscosity model of Launder-Sharma with the inclusion of the buoyancy terms in the energy equation. This model has been used for greater stability and superior results for blockage flow as reported by Draco et al. 2012 [29, 26] and Mathur and He [30].

Systematic grid dependency tests were carried out in all cases of blockages proximity and empty enclosure. The final y-plus (y^+) results are presented in Figure 8(a-d). All the simulations conducted in this paper were performed with y-plus value less than 0.50 for the blockages and y-plus value less than 0.7 for all horizontal and vertical walls. It is worthwhile to note that the process of computing a steady-state solution using very fine mesh has been quite challenging because of the oscillations associated with higher-order discretization schemes. As a result, a number of steps were taken to achieve a steady-state solution. Initially, low value of Rayleigh number (10^6) was adopted for the solution using an incompressible unsteady solver with a time step of 0.002s with the first-order scheme for convection terms. The resulting data files for the three cases were then used as an initial guess for the higher Rayleigh number simulation using the higher-order discretization schemes. This method helped to create a more realistic initial field for the LRKE runs. Thermal properties of the working air were estimated at the mean temperature of the isothermal walls (44.4 ^{0}C) of the cavity.

The wall's thermal condition used in the numerical calculation was similar to the experimental data reported earlier in this paper, and the thermal properties are summarised in Table 2.The dry air properties were evaluated using the average temperature (=42.2 °C) of the hot and cold wall. The experimental thermal boundary condition shown in Figure 5 was used for the top and bottom walls and was incorporated into FLUENT through the User-Defined-Function. The hot and cold walls were set at 65.5 ±0.8 °C and 23.3 ±0.8 °C respectively.

Table 2: Thermal properties of air and materials

Density (kg/m³)	Boussinesq (=1.12)
Specific heat (J/kg-K)	1.01×10^3
Thermal conductivity (W/m-K)	0.0272
Viscosity (kg/m-s)	1.92×10^{-5}
Thermal expansion coefficient (1/K)	3.17×10^{-3}
Prandtl number	0.712

Finally, to simulate the heat transfer due to radiation, the Discrete Ordinate (DO) method has been chosen due to its proven superiority in predicting radiative heat transfer as reported by Versteeg and Malalasekera [31] and Draco et al. 2012 [29]. The angular discretisation parameters used in the simulations are 2 and 6 in the Theta and Phi directions respectively.

5.1 Profiles of wall y-plus (y^+) distributions

The y-plus distributions along all four walls are presented in Figure 8(a-d).

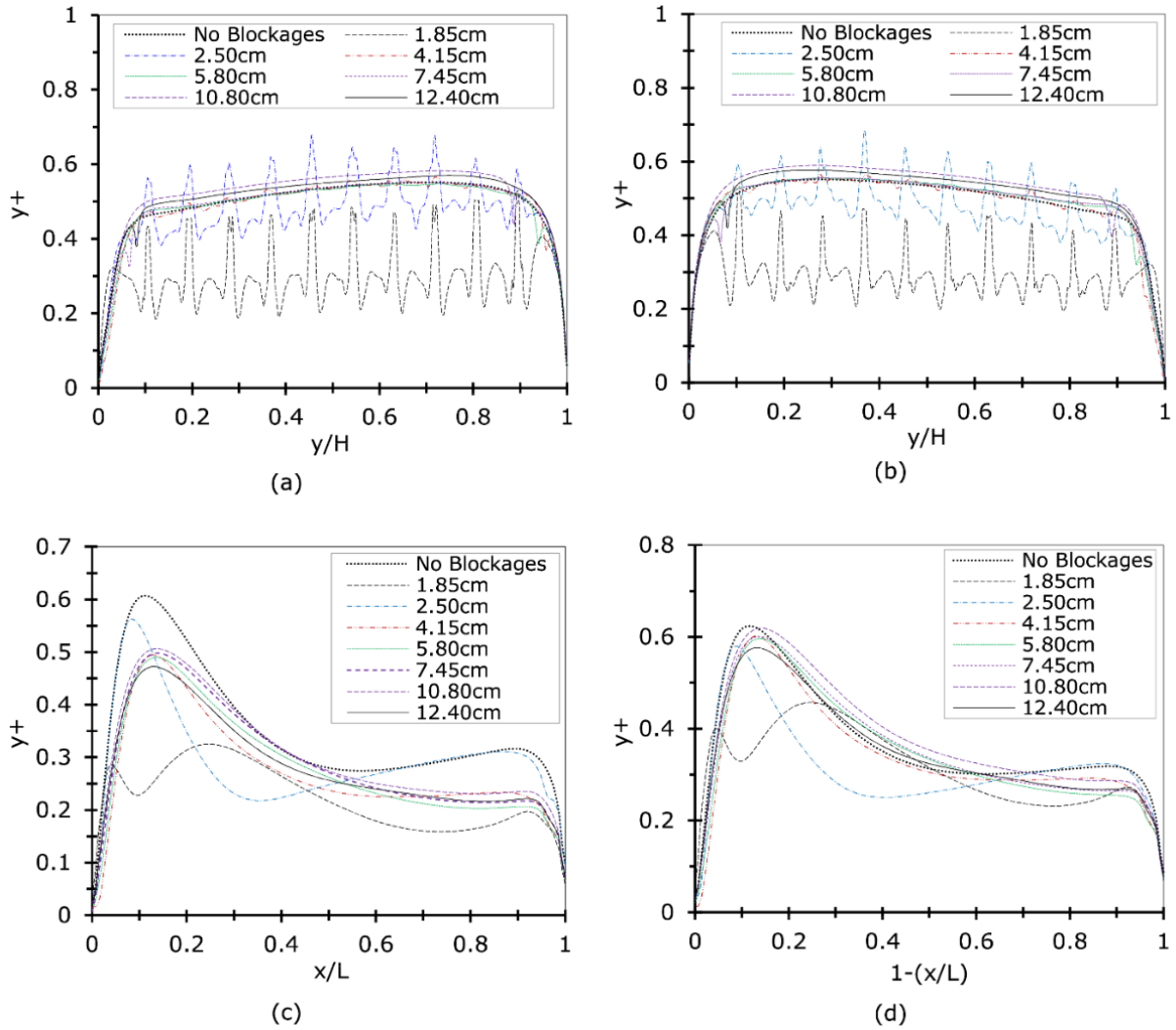

Figure 8: wall y^+ at (a) cold wall (b) hot wall (c) top wall (d) bottom wall

5.2 Comparison between experimental and numerical results

The experimental temperature data have been validated using the results from the numerical simulation and presented in Figure 9(a-d).

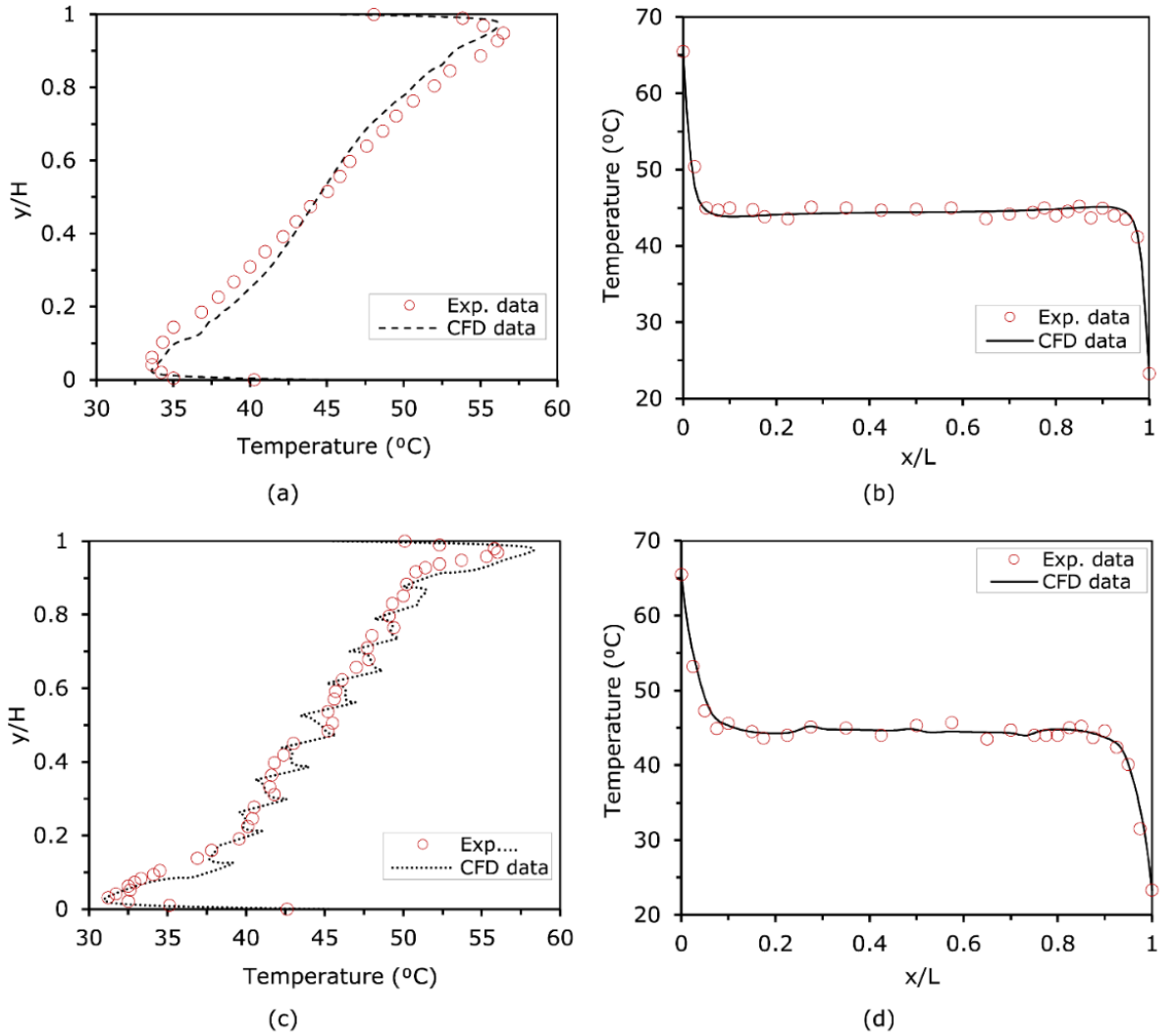

Figure 9: experimental temperature data comparison with numerical results at (a) mid-width of empty box (b) mid-height of empty box (c) mid-width for blockages-wall proximity δ= 2.5 cm (d) mid-height for blockages-wall proximity δ= 2.5 cm

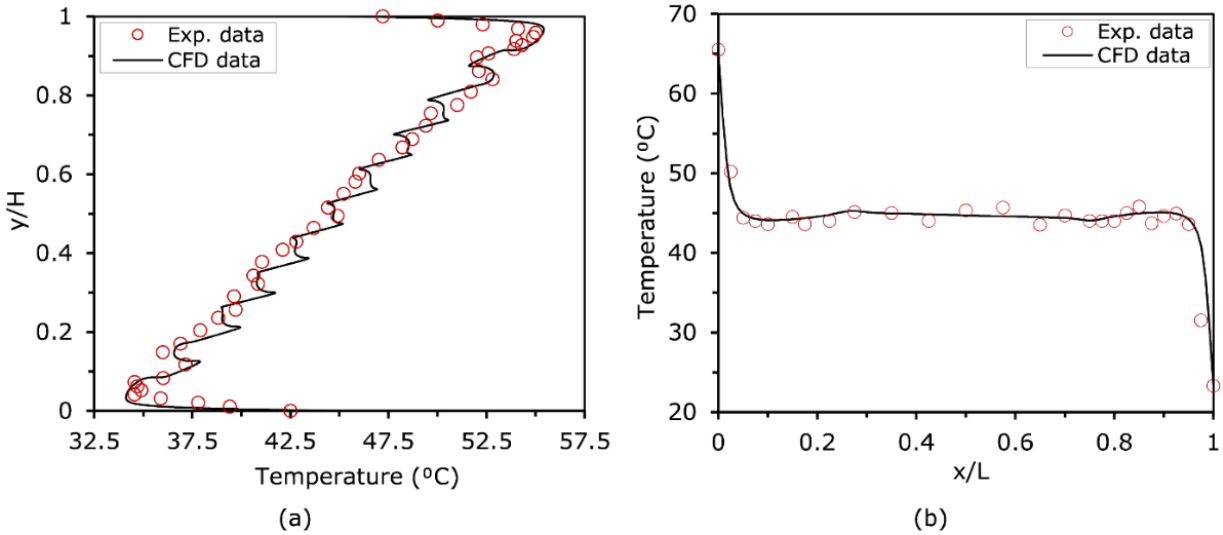

Figure 10: experimental temperature data comparison with numerical results at (a) mid-width for blockages-wall proximity δ= 10.8 cm (b) mid-height for blockages-wall proximity δ= 10.8 cm.

5.3 *Effect of blockage-wall proximity on flow and temperature fields*

The numerical results of the air velocity, temperature and wall heat flux collated at various positions inside the rectangular enclosure for varying blockages proximity from the vertical active walls are presented in this section. The result of the enclosure without blockages was used as a reference data to better understand the influence of varying the blockages proximity from the active vertical walls. Figure 11(a) shows the vertical velocity profiles at the mid-height of enclosure with and without blockages, with Figure 11(b) to Figure 11(b-c) showing the velocity profile at 0.043m from bottom and top walls respectively. It can be observed that in all cases, the flow at the core region is almost stagnant.

The influence of the blockages proximity on the flow is more significant near the top and bottom as shown by the peaks of the velocity boundary profiles in Figure 11(b) and Figure 11(c) respectively. It is observed that the blockages proximity of 1.85 cm has the most influence on the profile of the hydrodynamic boundary layer near the vertical active wall. This is as a result of the blockages location within the wall hydrodynamic boundary layer (which has been estimated to be about 2 cm) and thereby interacting or suppressing/blocking the flow. The peak of the vertical velocity profiles near the bottom of the cold wall and near the top of the hot wall is mostly affected by the change in the proximity values as shown in Figure 11(b) and Figure 11 respectively. Figure 11(d) further shows the effect of proximity on the horizontal velocity profile at mid-width near the top and bottom walls of the cavity. In general, when the blockages are placed very close to the vertical active walls in such a way that it interacts with the hydrodynamic boundary layer, the local buoyancy force acting on the flow in the boundary layer travelling along the vertical walls is suppressed. The influence of the blockages-wall proximity on the flow velocity and turbulent intensity are further shown as 2D contours in Figure 12(a) and Figure 12(b) respectively.

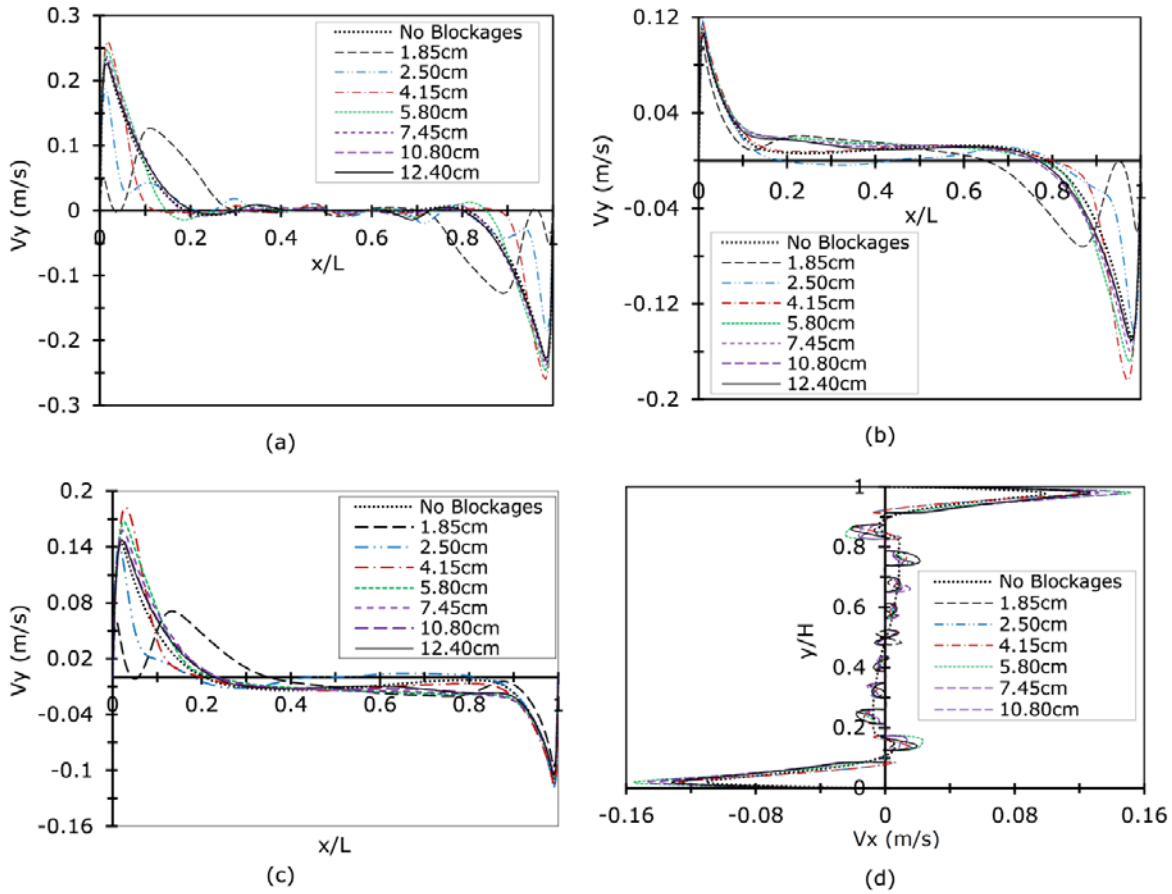

Figure 11: velocity profiles comparison for all blockages-wall proximity at (a) mid-height (b) 0.043 m from bottom (c) 0.043 m from top wall and (d) mid-width

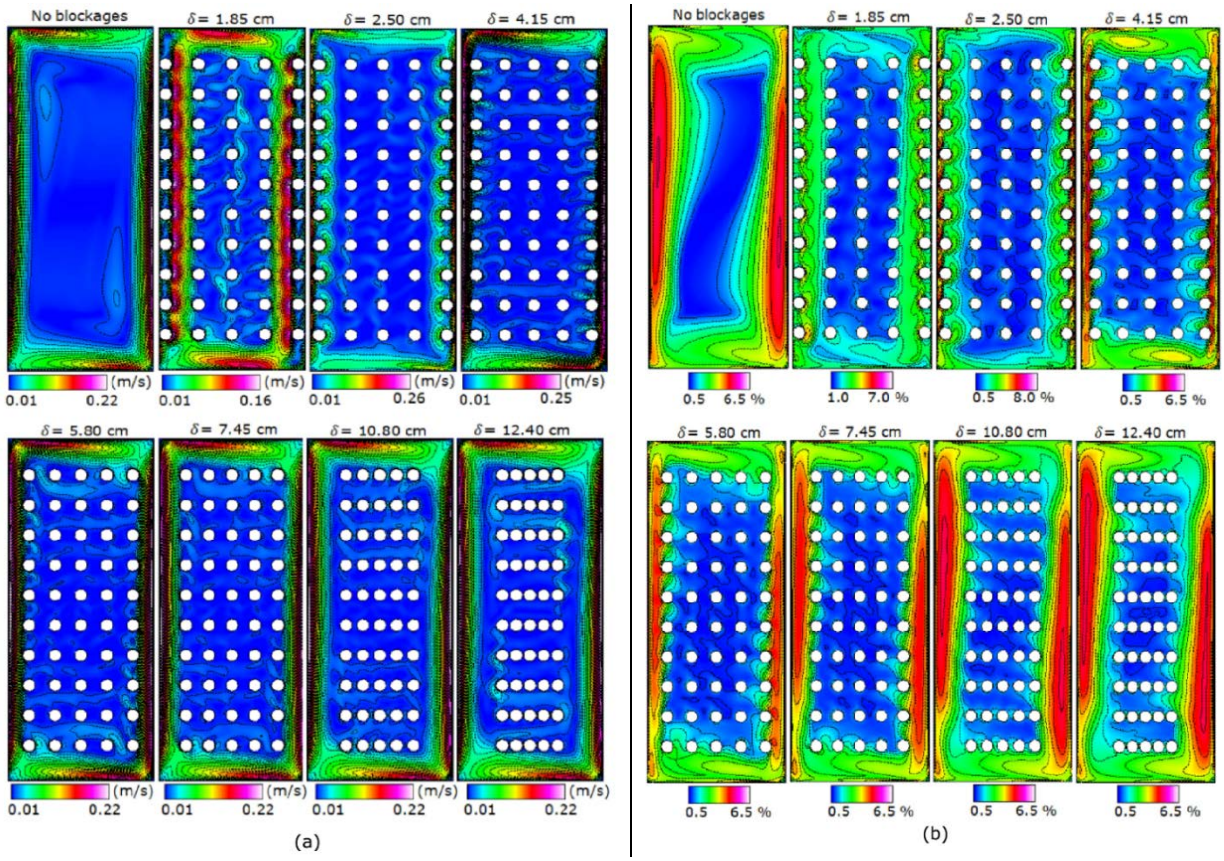

Figure 12: Contour of (a) velocity magnitude comparison (b) turbulent intensity comparison

The vertical temperature distributions at mid-height and at 0.043 m from the top and bottom walls are represented in Figure 13(a), Figure 13(b) and Figure 13(c) respectively, for enclosures with and without blockages. The temperature profiles in the core region of the enclosures displays linear variation which indicates that only a small portion of heat is transferred by molecular conduction across the core of the cavity as shown in Figure 13(a). For blockages positioned within the hydrodynamic boundary layer give a much larger slope of temperature profile along the horizontal distance in regions near the vertical walls. Since the temperature profiles of blockages positioned outside the hydrodynamic boundary layer are approximately uniform, it indicates that there is insignificant influence on the natural convection flow. The influence of blockages proximity is more visible at regions near the top and bottom wall of the enclosure. Figure 13(b) and Figure 13(c) shows the vertical temperature profile distributions evaluated at 0.043 m from top and bottom walls of the enclosure. It can be observed that at the top and bottom wall regions, about 11.0% reduction or increment in temperature is possible depending on the proximity of the blockages from the vertical active wall. Further comparison of the temperature distribution for the various cases of blockages proximity is shown in Figure 14.

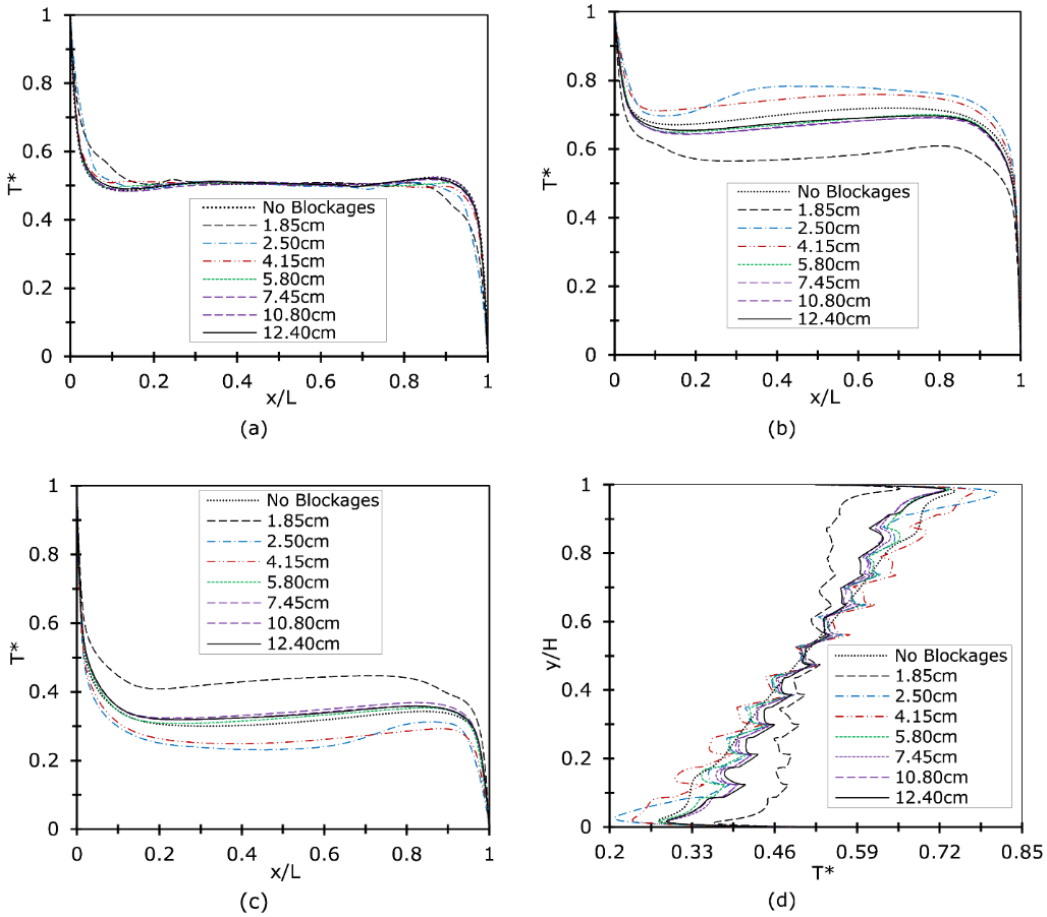

Figure 13: temperature profiles comparison for all blockages-wall proximity at (a) mid-height (b) 0.043 m from top wall (c) 0.043 m from bottom wall (d) mid-width

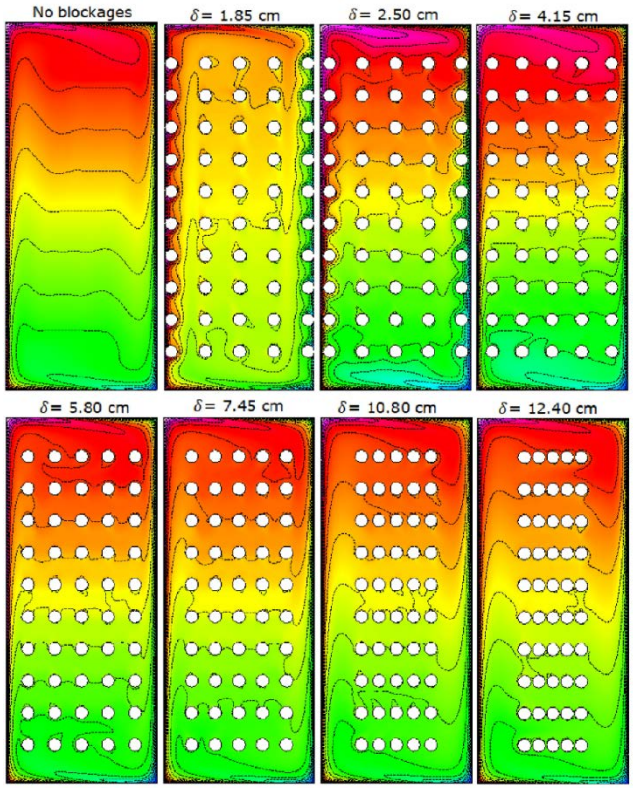

Figure 14: temperature contours comparison

5.4 *Wall heat transfer coefficients*

To investigate the wall heat transfer coefficients, the local and average Nusselt number values were evaluated using Eq.(2) and Eq.(3), respectively.

$$Nu = \frac{Q_i L}{\bar{k}\left(T_h - T_c\right)} \tag{2}$$

$$\overline{Nu} = \frac{\overline{Q} L}{\bar{k}\left(T_h - T_c\right)} \tag{3}$$

$$\% \, \Delta \overline{Nu} = \frac{\overline{Nu}_{\delta} - \overline{Nu}_{f}}{\overline{Nu}_{f}} \times 100\% \tag{4}$$

Where, Q_i represents the local heat flux evaluated at each node along a given wall, $\overline{Q}$ is the integral average wall heat flux, L is the width of the cavity $(L = H, \text{height})$, $\bar{k}$ is the average fluid thermal conductivity, the subscripts δ and f represents enclosure blockages proximity and enclosure without blockages respectively.

Figure 15(a-d) show the influence of the blockages proximity on the local Nusselt number distributions for all walls. It can be observed that the blockages proximity affects the wall heat transfer and its influence become very significant when the blockages are positioned very close to the active walls in such a way that it is fully within the hydrodynamic boundary layer. The proximity value used in this study show values less than 2.50 cm have a significant influence on the wall heat transfer, while the proximity values from 4.15 cm have minimal influence on the wall heat transfer. For both active vertical walls, the influence of blockages proximity becomes maximum at regions near the top wall when compared to those near the bottom wall as shown in Figure 15(a) and Figure 15(b). As expected, the profiles of the local heat transfer along the top wall (Figure 13) show higher peaks near the hot wall (where heat enters the enclosure) and lower peaks near the cold wall (where heat leaves the enclosure). The influence of blockages are also shown to be significant especially when the blockages have full or partial interaction with the hydrodynamic boundary layer along the vertical walls. From this study, it can be observed that reduction in heat entering or leaving the cavity from the vertical walls is possible with blockages proximity of 1.85 cm. Also, at the top and bottom walls, reduction in heat transfer is possible with 1.85 cm proximity, but increment in heat transfer with the same amount can be achieved with 4.15 cm proximity value.

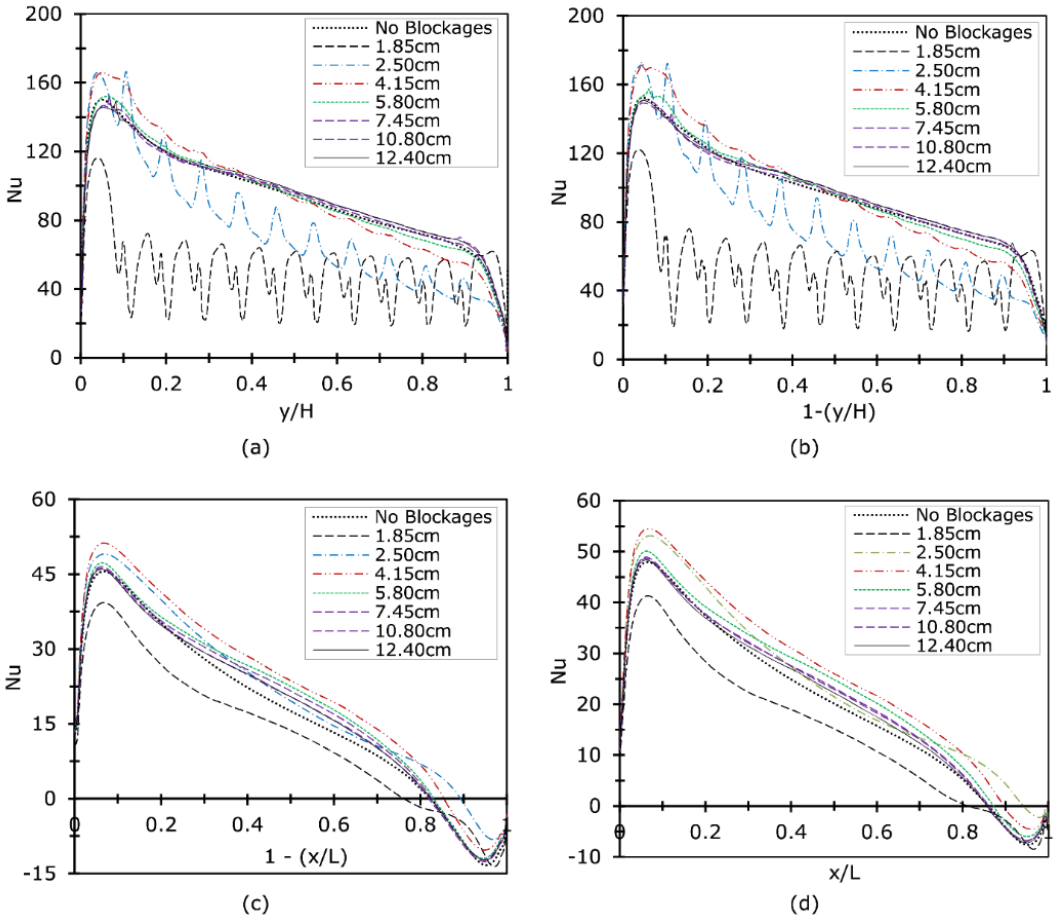

Figure 15: Local Nusselt number along (a) hot wall (b) cold wall (c) top wall (d) bottom wall

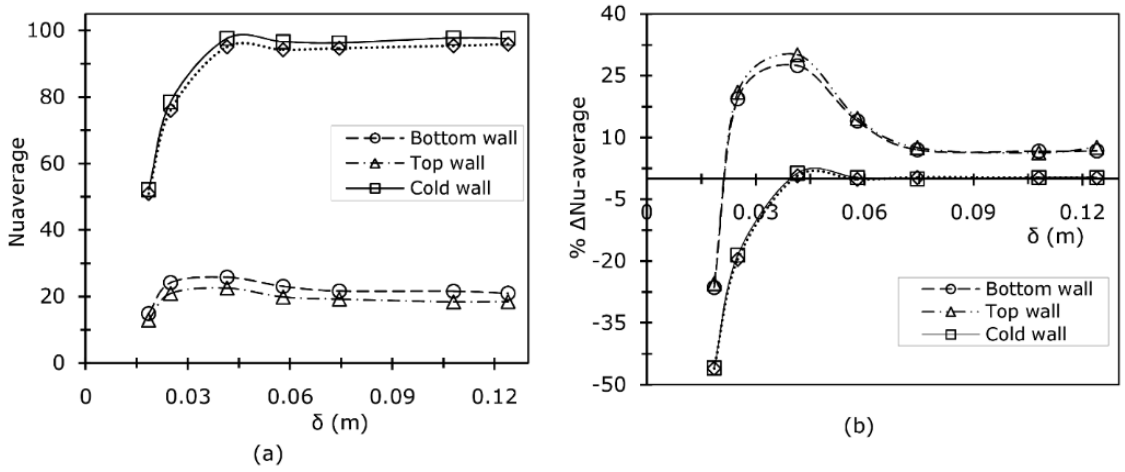

Figure 16: wall heat transfer coefficient (a) average Nusselt number at all walls (b) percentage change in average Nusselt number for varying blockages-wall proximity

Wall average Nusselt number at each wall was also evaluated and plotted (Figure 16a) as a function of blockages proximity. It can be observed that for proximity values very close to the wall resulted in a reduction in the wall heat transfer due to the blockage effect as stated earlier. However, as the blockages are positioned outside the hydrodynamic boundary layer, its influence on the wall heat transfer is insignificant. The influence of varying blockages proximity as percentage change in average Nusselt number shown in

Figure 16(b) was evaluated using Eq.(4). It can be observed that by varying blockages proximity, it is possible to have a reduction of the natural convection heat transfer. When the blockages were located at 1.85 cm from the vertical walls, the heat transfer was reduced by about 26.4% and 46.0% of the vertical and horizontal walls respectively. This reduction was lower as the proximity value increases, with proximity values of 2.50 cm and 4.15 cm resulted in 20.97% and 30.1% increment respectively at vertical walls. Proximity value of 4.15 cm provided the optimum increment in the heat transfer. However, at the vertical wall proximity values greater than 7.45 cm results in a constant increment of about 7.6% and no change in the percentage average heat transfer. For the horizontal walls, there are no significant changes with proximity values greater than 4.15 cm.

6.0 **Conclusions**

A thermal test rig capable of establishing a two dimensional natural convection flow was designed and validated to supply temperature data at various locations within the enclosure. The experimental data were also verified by numerical investigations. The reliable experimental temperature data provided will enhance the development and validation of computational codes for low turbulence natural convection flow in an enclosed space with and without isolated blockages. Numerical study was conducted to provide further flow and wall heat transfer data in order to adequately quantify and analyze the influence of blockages proximity from the vertical walls. From the results and discussions, the following conclusion can be drawn:

a) The experiments were conducted with high level of accuracy and the generated temperature data compared well with numerical results. Hence the results can form experimental benchmark temperature data which will be useful for validation of CFD codes relating to low turbulence natural convection heat transfer in enclosures partially filled with isolated solid objects.
b) Blockages proximity can be seen to affect the overall heat transfer via flow field. The fact that the variation of the proximity of an isolated solid object from the vertical walls influences the scenario drastically is a vindication that the proximity of objects near vertical walls does play a significant role in apparently low temperature applications.
c) The effect of blockages position within the hydrodynamic boundary layer could result in about 11% variation in air temperature near the horizontal wall region. Additionally, a reduction of 26.4% and 46% in the percentage average heat transfer coefficient were observed at the vertical and horizontal walls respectively.
d) Increment of about 7.6% in the percentage average heat transfer coefficient is obtained when the blockages proximity is positioned outside the active wall hydrodynamic boundary layer.
e) It can hence be argued that isolated object proximity from the active vertical wall in buoyancy driven flow can be an important factor when designing such applications.

References

[1] S. Kadem, A. Lachemet, R. Younsi and D. Kocaefe, "3d-Transient modeling of heat and mass transfer during heat treatment of wood," *International Communications in Heat and Mass Transfer,* vol. 38, no. 6, pp. 717-722, 2011.

[2] O. Laguerre, A. S. Ben and D. Flick, "Experimental study of heat transfer by natural convection in a closed cavity: application in a domestic refrigerator," *Journal of Food Engineering,* vol. 70, no. 14, pp. 523-537, 2005.

[3] O. Laguerre, S. Benamara, D. Remy, Flick and D., "Experimental and numerical study of heat and moisture transfers by natural convection in a cavity filled with solid obstacles," *International Journal of Heat and Mass Transfer,* vol. 52, no. 25–26, pp. 5691-5700, 2009.

[4] O. Laguerre and D. Flick, "Heat transfer by natural convection in domestic refrigerators," *Journal of Food Engineering,* vol. 62, no. 1, pp. 79-88, 2004.

[5] S. Salat, P. Xin, A. Joubert, F. Sergent, P. Penot and L. Quéré, "Experimental and numerical investigation of turbulent natural convection in a large air-filled cavity," *International Journal of Heat and Fluid Flow,* vol. 25, no. 5, pp. 824-832, 2004.

[6] Y. Tian and T. Karayiannis, "Low turbulence natural convection in an air filled square cavity Part I: The thermal and fluid flow fields," *International Journal of Heat and Mass Transfer,* vol. 43, no. 6, pp. 849-866, 2000.

[7] Y. Tian and T. Karayiannis, "Low turbulence natural convection in an air filled square cavity - Part II: the turbulence quantities," *International Journal of Heat and Mass Transfer,* vol. 43, no. 6, pp. 867-884, 2000.

[8] T. K. F. Ampofo, "Experimental benchmark data for turbulent natural convection in an air filled square cavity," *International Journal of Heat and Mass Transfer,* vol. 46, no. 19, pp. 3551-3572, 2003.

[9] A. A. Dafa'Alla and P. L. Betts, "Experimental study of turbulent natural convection in a tall air cavity," *Experimental Heat Transfer:A Journal of Thermal Energy Generation, Transport, Storage, and Conversion,* pp. 165-194, 1996.

[10] P. François, S. Olivier and S. Didier, "Preliminary experiments on the control of natural convection in differentially-heated cavities," *International Journal of Thermal Sciences,* vol. 49, no. 10, 2010.

[11] W. L. Wei Chen, "Numerical and experimental analysis of convection heat transfer in passive solar heating room with greenhouse and heat storage," *Solar Energy,* vol. 76, no. 5, pp. 623-633, 2004.

[12] S. Didier, R. Nicolas, D. Francis and P. François, "Natural convection in an air-filled cavity: Experimental results at large Rayleigh numbers," *International Communications in Heat and Mass Transfer,* vol. 38, no. 6, pp. 679-687, 2011.

[13] F. Ampofo and T. G. Karayiannis, "Experimental benchmark data for turbulent natural convection in an air filled square cavity," *International Journal of Heat and Mass Transfer,* vol. 46, no. 19, pp. 3551-3572, 2003.

[14] G. Barakos, E. Mitsoulis and D. Assimacopoulos, "Natural convection flow in a square cavity revisited: Laminar and turbulent models with wall functions," *International Journal for Numerical Methods in Fluids,* vol. 18, no. 7, pp. 695-719, 1994.

[15] O. Laguerre, A. S. Ben, G. Alvarez and D. Flick, "Transient heat transfer by free convection in a packed bed of spheres: Comparison between two modelling approaches and experimental results," *Applied Thermal Engineering,* vol. 28, no. 1, pp. 14-24, 2008.

[16] D. J. Braga and M. J. D. Lemos, "Laminar natural convection in cavities filled with circular and square rods," *International Communications in Heat and Mass Transfer,* vol. 32, no. 10, pp. 1289-1297, 2005.

[17] K. Hooman and A. A. Merrikh, "Theoretical Analysis of Natural Convection in an Enclosure Filled with Disconnected Conducting Square Solid Blocks," *Transport in Porous Media,* vol. 85, no. 2, p. 641–651, 2010.

[18] P. Nithiarasu, K. Seetharamu and T. Sundararajan, "Natural convective heat transfer in a fluid saturated variable porosity medium," *International Journal of Heat and Mass Transfer,* vol. 40, no. 16, pp. 3955-3967, 1997.

[19] M. K. Das, K. Reddy and K. Saran, "Conjugate natural convection heat transfer in an inclined square cavity containing a conducting block," *International Journal of Heat and Mass Transfer,* vol. 49, no. 25–26, pp. 4987-5000, 2006.

[20] T. Basak, S. Roy, T. Paul and I. Pop, "Natural convection in a square cavity filled with a porous medium: Effects of various thermal boundary conditions," *International Journal of Heat and Mass Transfe,* vol. 49, no. 7–8, pp. 1430-1441, 2006.

[21] G. Desrayaud and G. Lauriat, "Heat and mass transfer analogy for condensation of humid air in a vertical channel," *Heat and Mass Transfer,* vol. 37, no. 1, p. 67–76, 2001.

[22] H. Yoon, D. Yu, M. Ha and Y. Park, "Three-dimensional natural convection in an enclosure with a sphere at different vertical locations," *International Journal of Heat and Mass Transfer,* vol. 53, no. 15–16,, pp. 3143-3155, 2010.

[23] E. J. Braga and M. J. Lemos, "Heat transfer in enclosures having a fixed amount of solid material simulated with heterogeneous and homogeneous models," *International Journal of Heat and Mass Transfer,* vol. 48, no. 23-24, pp. 4748-4765, 2005.

[24] B. Calcagni, F. F.Marsili and M. Paroncini, "Natural convective heat transfer in square enclosures heated from below," *Applied Thermal Engineering,* vol. 25, no. 16, pp. 2522-2531, 2005.

[25] A. Merrikh and J. Lage, "Natural convection in an enclosure with disconnected and conducting solid blocks," *International Journal of Heat and Mass Transfer,* vol. 48, no. 7, pp. 1361-1372, 2005.

[26] D. Iyi, "A Study on Buoyancy Driven Turbulent Flow Associated with Radiation in Cavities Partially Filled with Blockages," Doctoral thesis: Northumbria University, Newcastle upon Tyne, 2013.

[27] P. L. Betts and I. H. Bokhari, "Experiments on turbulent natural convection in an enclosed tall cavity," *International Journal of Heat and Fluid Flow,* vol. 21, no. 6, pp. 675-683, 2000.

[28] *ANSYS Academic Research Fluent, Release 14.0,* 2011.

[29] D. Iyi, R. Hasan and R. Penlington, "Interaction effects between surface radiation and double-diffusive turbulent natural convection in an enclosed cavity filled with solid obstacles," in *ICHMT International Symposium on Advances in Computational Heat Transfer*, Bath, England, 2012.

[30] A. Mathur and S. He, "Performance and implementation of the Launder-Sharma low-Reynolds number turbulence model," *Computer & Fluid,* vol. 79, no. 25, pp. 134-139, 2013.

[31] H. K. Versteeg and W. Malalasekera, An Introduction to Computational Fluid Dynamics: The Finite Volume Method, 2nd ed., Essex: Pearson Education Limited, 2007.

[32] N. Tomás and S. Da-Wen, "Computational fluid dynamics (CFD) – an effective and efficient design and analysis tool for the food industry: A review," *Trends in Food Science & Technology,* vol. 17, no. 11, pp. 600-620, 2006.

[33] X. Bin and S. Da-Wen, "Applications of computational fluid dynamics in the food industry: a review," *Computers and Electronics in Agriculture,* vol. 34, no. 1, pp. 5-24, 2002.

[34] B. Launder and D. B. Spalding, "The numerical computation of turbulent flows," *Computer Methods in Applied Mechanics and Engineering,* vol. 3, no. 2, pp. 269-289, 1974.

[35] R. Henkes and C. J. Hoogendoorn, "Comparison of turbulence models for the natural convection boundary layer along a heated vertical plate," *Int. J. Heat Mass Transfer,* vol. 32, pp. 157-169, 1989.

[36] V. C. Patel, W. Rodi and G. Scheuerer, "Turbulence models for near-wall and low Reynolds number flows - A review," *AIAA Journal,* vol. 23, no. 9, pp. 1308-1319, 1985.

[37] B. Launder and B. Sharma, "Application of the energy-dissipation of turbulence to calculation of low near a spinning disc," *Lett Heat Mass Transfer,* vol. 1, pp. 131-138, 1974.

[38] J. H. Ferziger and M. Peric, Computational Methods for Fluid Dynamics, New York, USA: Springer, 2002.

[39] A. Mathur and S. He, "Performance and Implimentation of Launder-Sharma Low-Reynolds number Turbulence Model," *Computer and Fluids,* vol. 79, pp. 134-139, 2013.

[40] S. Chandrasekhar, Radiative transfer, New York: Dover Publications, 1960.

[41] R. Siegel and J. Howell, Thermal radiation heat transfer, 4th ed., London: Taylor & Francis, 2002.

[42] D. Iyi, R. Hasan and R. Penlington, "Effect of Emissivity on the Heat and Mass Transfer of Humid Air in a Cavity Filled with Solid Obstacles," *Numerical Heat Transfer, Part A: Applications - An International Journal of Computation and Methodology,* vol. 67, no. 5, pp. 531-546, 2014.